



# Analyzing the PMIP4-CMIP6 ensemble: a workflow and tool (`pmip_p2fvar_analyzer v1`)

Anni Zhao<sup>1</sup>, Chris M. Brierley<sup>1</sup>, Zhiyi Jiang<sup>1</sup>, Rachel Eyles<sup>1</sup>, Damián Oyarzún<sup>1</sup>, and Jose Gomez-Dans<sup>1</sup>

<sup>1</sup>Dept of Geography, University College London, London, WC1E 6BT, UK

**Correspondence:** Anni Zhao (anni.zhao.16@ucl.ac.uk)

**Abstract.** Experiment outputs are now available from the Coupled Model Intercomparison Project's 6<sup>th</sup> phase (CMIP6) and the past climate experiments defined in the Model Intercomparison Project's 4<sup>th</sup> phase (PMIP4). All of this output is freely available from the Earth System Grid Federation (ESGF). Yet there are overheads in analysing this resource that may prove complicated or prohibitive. Here we document the steps taken by ourselves to produce ensemble analyses covering past and future simulations. We outline the strategy used to curate, adjust the monthly calendar aggregation and process the information downloaded from the ESGF. The results of these steps were used to perform analysis for several of the initial publications arising from PMIP4. We provide post-processed fields for each simulation, such as climatologies and common measures of variability. Example scripts used to visualise and analyse these fields is provided for several important case studies.

## 1 Introduction

Paleoclimate modelling has long been used to understand the mechanisms of past climate changes, and also has served as a tool to test the out-of-sample boundary conditions and forcings like high atmospheric CO<sub>2</sub> concentration that are used in future climate change projections (e.g. Harrison et al., 2014, 2015; Schmidt et al., 2014). The Paleoclimate Model Intercomparison Project, now in its fourth phase (PMIP4; Kageyama et al., 2018) is a project endorsed by the Coupled Model Intercomparison Project phase 6 (CMIP6; Eyring et al., 2016), which aims to analyse and understand the differences between model simulations of past climates. PMIP4 has been updated from its earlier phase PMIP3 (Braconnot et al., 2012) by including additional past warm periods (Fig. 1) and running improved forcings and boundary conditions by the new generation of climate models (Kageyama et al., 2018; Eyring et al., 2016).

The mid-Holocene (6000 years ago) and the Last Interglacial (127,000 years ago) are characterised by altered seasonal and latitudinal distribution of incoming solar radiation when the Earth's orbits were different from modern. The *midHolocene* and *lig127k* experiments are Tier 1 PMIP4-CMIP6 simulations (Fig. 1); designed to examine the model response to changes in the Earth's orbit in periods when the atmospheric greenhouse gas concentrations were similar to the preindustrial level and the topographies were also similar to modern. Otto-Bliesner et al. (2017) described the protocols and specific information for the two experiments in detail. Brierley et al. (2020) summarised the large features in the PMIP4-CMIP6 *midHolocene* simulations and the changes since the PMIP3-CMIP5 generation. Features in the PMIP4-CMIP6 *lig127k* ensemble have been analysed by

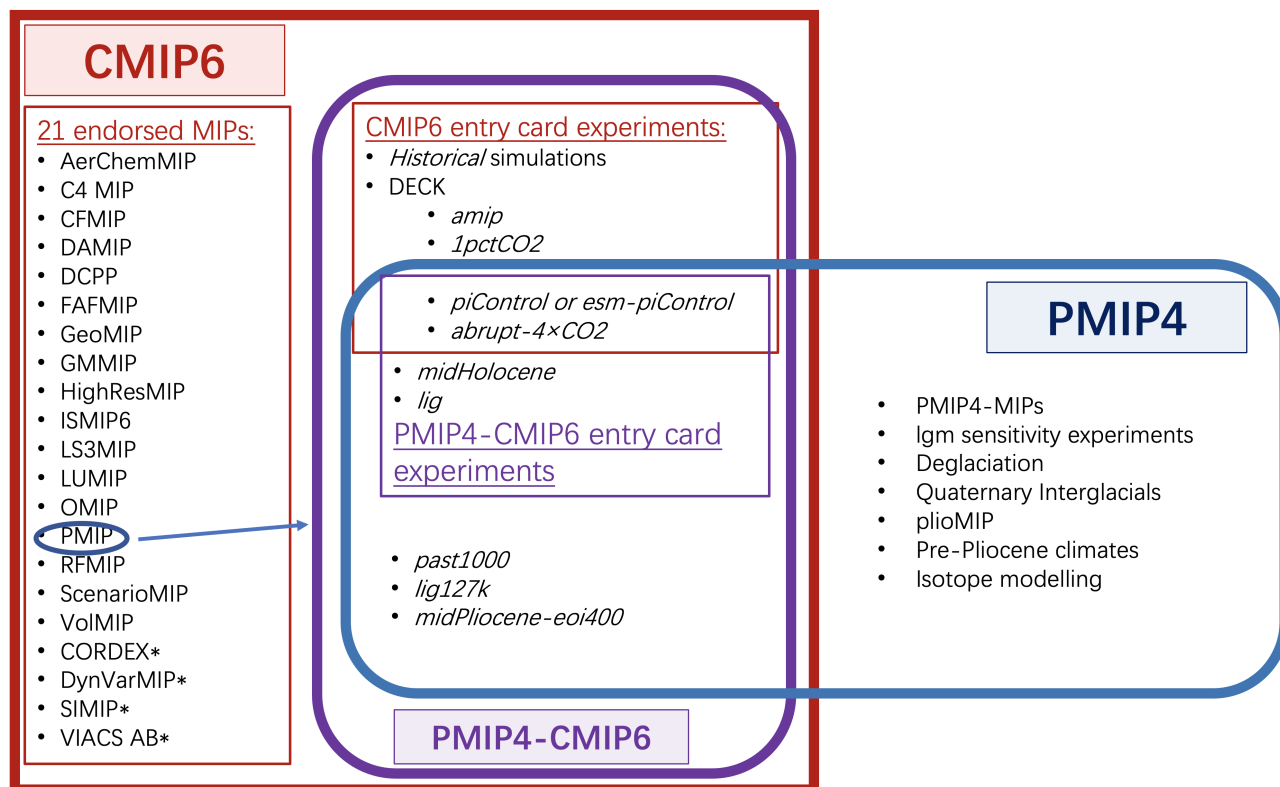


**Figure 1. Schematic diagram illustrating the PMIP4-CMIP6 experiments and their relationship to CMIP6 and PMIP4, according to Eyring et al. (2016) and Kageyama et al. (2018)**

Otto-Bliesner et al. (2021). These two ensembles within PMIP4 have contributed to the text in several chapters (Gulev et al., 2021; Eyring et al., 2021; Douville et al., 2021; Fox-Kemper et al., 2021) in the latest Sixth Assessment Report (AR6) of the Intergovernmental Panel on Climate Change (IPCC), as well as figures (Eyring et al., 2021) .

30 Here we provide a detailed description of the workflow and scripts that have been used to create figures in the primary description papers of the latest PMIP4-CMIP6 *midHolocene* (Brierley et al., 2020) and *lig127k* (Otto-Bliesner et al., 2021) experiments. The scripts have also been used for figures in past2future multi-experiment papers on the PMIP3-CMIP5 tropical Atlantic inter-annual variability (Brierley and Wainer, 2018), PMIP3-CMIP5/6 climate variability (Rehfeld et al., 2020) and PMIP3-CMIP5 and PMIP4-CMIP6 ENSO (Brown et al., 2020) and contributed to Figures 3.2b and 3.11 in IPCC AR6 WG1

35 Chapter 3 (Eyring et al., 2021). In section 2, we give a description of the PMIP4 output availability and a discussion of how to access data, along with an evaluation of how and when to apply the `PaleoCalAdjust` software. The following section describes the Climate Variability Diagnostics Package (CVDP) and how it has been modified for PMIP4 purposed. The general



**Table 1.** List of variables in the *piControl*, *midHolocene* and *lig127k* simulations that were downloaded from the ESGF.

Long name	Variable name	Unit	Table ID
Near-Surface Air Temperature	tas	K	Amon
Surface Temperature	ts	K	Amon
Sea Level Pressure	psl	Pa	Amon
Precipitation	pr	kg m <sup>-2</sup> s <sup>-1</sup>	Amon
Ocean Y Overturning Mass Streamfunction	msftyz	kg s <sup>-1</sup>	Omon
Sea-Ice Area Percentage (Ocean Grid)	siconc	%	SImon

Information follows

[http://proj.badc.rl.ac.uk/svn/exarch/CMIP6dreq/tags/latest/dreqPy/docs/CMIP6\\_MIP\\_tables.xlsx](http://proj.badc.rl.ac.uk/svn/exarch/CMIP6dreq/tags/latest/dreqPy/docs/CMIP6_MIP_tables.xlsx)

NCL and python routines (as `pmip_p2fvar_analyzer v1.0`) used in the above papers are described in detail in section 4. Some case studies of possible analyses using the described workflow are given in section 5, followed by a short summary in section

40 6.

## 2 Curating and Collating PMIP4 output

Each model participating in the CMIP6 has uploaded (or is going to) upload their DECK and historical simulations (and endorsed MIPs simulations if available) onto the Earth System Grid Federation (ESGF; Balaji et al., 2018, available at <https://esgf-node.llnl.gov/search/cmip6/>) in the standard format as required by the CMIP6 Data Request (Jukes et al., 2020). All CMIP6  
45 outputs have been written to netCDF files with one variable stored per file. Full lists of variables in the ESGF controlled vocabulary are available at [http://proj.badc.rl.ac.uk/svn/exarch/CMIP6dreq/tags/latest/dreqPy/docs/CMIP6\\_MIP\\_tables.xlsx](http://proj.badc.rl.ac.uk/svn/exarch/CMIP6dreq/tags/latest/dreqPy/docs/CMIP6_MIP_tables.xlsx). Users can restrict searching results by selecting appropriate search constraints (e.g. Variable, Experiment ID and Frequency). Table 1 lists the variables and their relevant information that we downloaded from the ESGF and used for analysis. For each PMIP  
50 was selected for each experiment. Only the FGOALS-g3 *midHolocene* has multiple runs, and `r1i1p1f1` has been selected. There are 4 different forcings available for the IPSL-CM6A-LR (Braconnot et al., 2019) : only the `r1i1p1f1` variant has been selected as that relates to the Tier 1 *midHolocene* protocol.

Since each experiment contained a single ensemble member, a revised database structure was adopted to harmonise both CMIP6 and CMIP5 ensemble conventions. The resulting database only has two directory levels: the top level is taken as the  
55 model, with a sub-directory for each experiment that contains all the outputs listed in Tab. 1. Additionally an ‘areacello’ fixed variable is stored in each sub-directory for the computation of sea ice area on rotated grids. These were not always deposited on the ESGF for an experiment and needed to be sourced from elsewhere. This curation approach has the added advantage of permitting manual treatment of individual issues. Symbolic links were used to populate this curated ESGF replica where



possible (to avoid the duplication of data files). When many little files were stored on the ESGF, these were concatenated in a single larger file (using `nrcat`) to avoid I/O bottlenecks. If output was available for varying years with a simulation, only the common years were used. This curation approach had the additional advantage permitting the inclusion of simulation prior to publication on ESGF, and allowed for a coherent treatment calendar-adjusted files. The file names of the resulting curated directory can be seen at [https://github.com/pmip4/UCL\\_curated\\_ESGF\\_replica](https://github.com/pmip4/UCL_curated_ESGF_replica).

The eccentricity, obliquity and precession at the mid-Holocene and the Last Interglacial were different from those at 1850 CE. Therefore aggregating up daily output to monthly averages using a 'fixed-length' calendar to define the number of days in each month is not appropriate across all the experiments: a 'fixed-angular' calendar should be used instead. Bartlein and Shafer (2019) provide a software, `PaleoCalAdjust`, to convert between the two calendars for simulation output that are produced and stored in general CMIP format. The process taken by the `PaleoCalAdjust` software is interpolate from non-adjusted monthly averages down to pseudo-daily values and then aggregate these values back up to a 'monthly' resolution for each 30° segments of the Earth's orbit (see `adjusted_month_lengths.xlsx` on Github for adjusted month lengths). Bartlein and Shafer (2019) evaluated the software's performance for monthly temperature and precipitation variations and showed that in some situations the aliases due to the calendar definition can be larger than the climate change signal. Therefore, Brierley et al. (2020) and Otto-Bliesner et al. (2021) decided to apply the the calendar adjustment when analysing seasonal temperature and precipitation. Regional mean temperature of the warmest month (MTWA) and of the coldest month (MTCO) for the mid-Holocene in Fig 3.44 in IPCC AR6 WG1 (Eyring et al., 2021) used adjusted monthly temperatures.

Brierley et al. (2020) explored the potential interpolation errors from `PaleoCalAdjust` on precipitation in monsoon regions (Pollard and Reusch, 2002) by analysing the averaged rain rate during the monsoon season over the South American monsoon domain in the IPSL-CM6A-LR *midHolocene*. As a result, Brierley et al. (2020) decided to not apply the calendar adjustment when analysing monsoon variables despite presenting DJF and JJA precipitation changes that did use it. In general, whether it is better to use `PaleoCalAdjust` depends on the steps in the subsequent processing and analysis. If scripts average many months without weighting by month length then we feel it is undesirable to use `PaleoCalAdjust`. This experience is summarised in the Fig. 2, which provides a recommendation of whether to deploy `PaleoCalAdjust` dependent on the proposed analyses. The monthly palaeoclimate plots in the IPCC Interactive Atlas (Gutierrez et al., 2021; Gutiérrez et al., 2021) are calendar adjusted, whilst the annual mean fields are computed as a unweighted average of the 12 un-adjusted monthly climatology (Brierley and Zhao, 2021a). This has the disadvantage that users will not be able recreate the annual mean themselves by downloading and averaging the 12 monthly fields, unless they weight them by the number of days in the month. Gutiérrez et al. (2021) also provide equivalent climatologies for the *midPliocene-eoi400* and *lig127k* ensembles. Subsetted files can be downloaded via the Interactive Atlas, although all the underlying files are also available (Brierley and Zhao, 2021a). It is worth noting that the ensembles available through these sources is only the subset of models who had uploaded output onto the ESGF. This difference is most marked for the *midPliocene-eoi400* and *lgm*, where images within the IPCC report (Gulev et al., 2021; Eyring et al., 2021) use the larger ensemble of Haywood et al. (2020) and ) that includes non-CMIP6 models. There may also be noticeable differences between PMIP4 *lgm* analysis contained within the report and the Atlas, because of the non-CMIP6 models included by Kageyama et al. (2021). All the analysis of the PMIP simulations discussed in the IPCC Report and its atlas

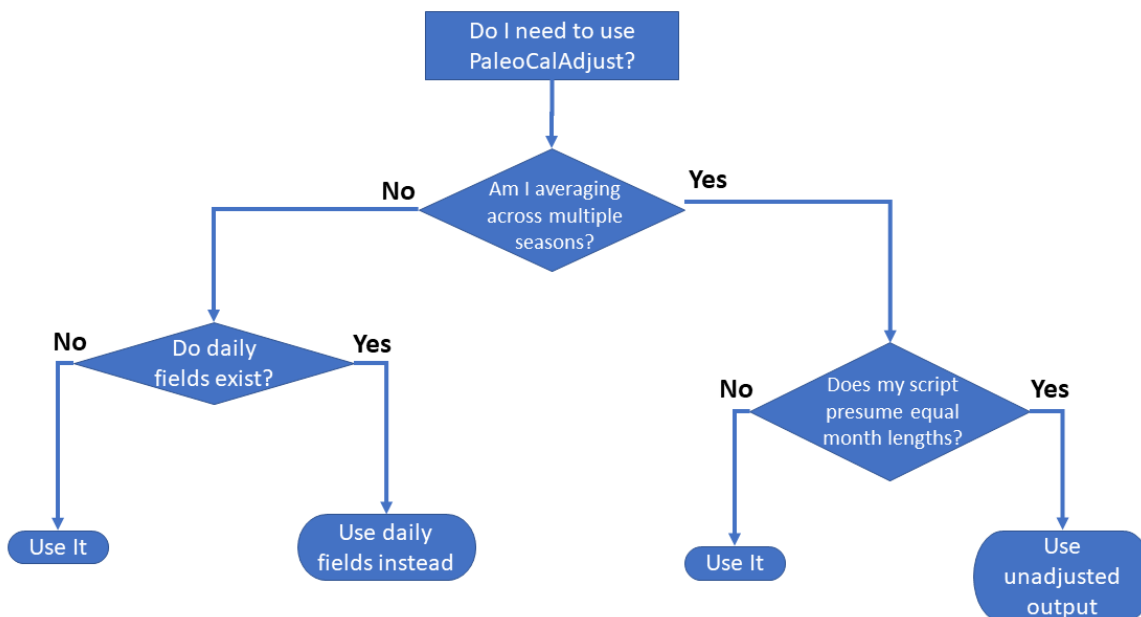


**Figure 2.** Flowchart summarising the processes used to determine whether it is desirable to deploy the PaleoCalAdjust software (developed by Bartlein and Shafer, 2019)

derive ensemble means by considering the models to have an equal weight. This is not the case for future projections in the  
95 report (e.g. Arias et al., 2021) – work is ongoing to determine appropriate weighting for palaeoclimate simulations (Schmidt  
et al., 2014) and the present workflow does not yet provide such functionality.

### 3 Post-processing of PMIP4 output

The Climate Variability Diagnostics Package (CVDP; Phillips et al., 2014) was developed by the National Center for Atmo-  
spheric Research (NCAR)’s Climate Analysis Section to improve and facilitate the evaluation of major modes of international  
100 climate variability, like El Niño-Southern Oscillation (ENSO) and Atlantic Multi-decadal Oscillation (AMO), in models and  
observations. This package computes time spatial patterns, standard deviation and trend maps, climatological fields, power  
spectra and time series of climate variabilities in any user-specified model simulations whose files fit CMIP5/CMIP6 out-  
put requirements. Analysis results of each model are presented via webpages including a summary table that contains model  
105 performance for key metrics of international variability shown as pattern correlations and RMSE compared to the chosen ob-  
servations. Outputs are saved in a netCDF file for later use, which contains the data fields that plotted in each png image. This



package has been used by Fasullo et al. (2020) to evaluate the representation of variability in the CMIP6. The resulting data along with the CVDP source code can be downloaded from <http://www2.cesm.ucar.edu/working-groups/cvcwg/cvdp>.

CVDP has been adapted for palaeoclimate purposes. Brierley and Wainer (2018) introduced additional coupled modes of variability in the Tropical Atlantic. Brown et al. (2020) altered the compositing of ENSO events to look throughout the year, not just DJF. Additionally, they computed La Niña and El Niño composites separately, although these were used in the publication. Otto-Bliesner et al. (2021) introduced the computation of time series of sea ice area, in addition to sea ice extent. Brierley et al. (2020) introduced the calculation of a global monsoon domain following the definition of Wang and Ding (2008); Wang et al. (2011, 2014) by applying two criteria as (a) annual range (local summer - local winter) of precipitation rate is greater than 2 mm d<sup>-1</sup> and (b) the local summer rainfall exceeds 55% of the annual total. The domain's extent is calculated separately for each individual monsoon season and its extent and area-averaged rain rate computed. This differs slightly from analyses of future projections, where the domain can be fixed at its present-day extent (Christensen et al., 2013). For regional monsoons, we follow the definition of regional monsoon in IPCC AR5 (Christensen et al., 2013) to compute the monsoon summer rain rate and areal extent for each of the seven regional monsoon. The monsoon diagnostics were also analysed by Otto-Bliesner et al. (2021).

In IPCC AR6, global monsoons in paleoclimate is presented in Chapter 3 Eyring et al. (2021), in which Fig 3.17 shows the global monsoon domain and intensity that is calculated as the ratio of (summer - winter) / (annual mean) for historical simulations. Notably, our criteria are different to the definitions used in the IPCC AR6 WG1 in which the global monsoon is defined as where the annual range of precipitation exceeds 2.5 mm/day as in Kitoh et al. (2013); IPCC (2021). Changes in regional monsoons are included in Chapter 8 (Douville et al., 2021) and Box TS13 Fig 1 (Arias et al., 2021) in IPCC AR6 WG1. However, regional monsoons in AR6 WG1 have been modified from AR5 WG1 which now are defined as six regional monsoons and two domains based on published literature and expert judgement (IPCC, 2021) rather than the seven regional land monsoons in the AR5 WG1 (Christensen et al., 2013) (see IPCC (2021) for details).

There are also some further modifications to the PMIP version of the CVDP package that have not been previously documented.

- The mean and standard deviation spatial fields are only computed over the years used to compute the climatology. This makes no difference unless a `custom_climo` is set (the default is to use all available years). It allows the climate state at a particular point in a transient simulation to be isolated, and is generally only used to select the end of the *abrupt4xco2* and *Ipctco2* experiments, or to select the satellite period in the *historical* experiment.
- The temperatures of the warmest month and the coldest month are computed, along with their (interannual) standard deviations. These are variables that are compiled from pollen-derived reconstructions (Bartlein et al., 2011). As the *mid-Holocene* comparison only features in the supplemental of Brierley et al. (2020), this modification was not documented in the manuscripts methodology.
- The principal-component based definition of the AMOC advocated by Danabasoglu et al. (2012) has been abandoned. We revert to a more-conventional definition: taking the AMOC as the maximum zonal mean streamfunction at 30°N



- 140 below 500m. This was originally motivated by the conflation of mean state changes and variability in the *past1000* simulations in the principal-component based definition. Whilst the maximum at 30°N can suffer similar issues, it is simpler to explain and diagnose them.
- Time series of area-average precipitation and surface air temperature are calculated for 58 regions. These consist of 30° latitude bands (over land and sea) as well as the climate regions presented in the IPCC report (AR5 regions; Collins et al., 2013). These time series are stored as variables named `ipcc_TLA_pr` and `ipcc_TLA_tas` respectively, where TLA is the conventional three letter acronym for the AR5 regions and a text string for the latitude bands. It is worth mentioning that currently the use of the present-day land-sea mask is hardwired into CVDP.
  - Monthly time series plots of the new monsoon and area-average diagnostics are written so that only a low resolution mean and spread are visualised for records greater than 150 years. This is more computationally efficient
  - 150 – The associated web pages have been altered to accommodate the new diagnostics

#### 4 Plotting post-processed outputs

A series of scripts have been developed that use the CVDP summary output files as inputs for ensemble analysis. Initial development of these scripts started was in NCL by Brierley and Wainer (2018) to complement the original package. Similar to CVDP, they consist of a library of common functions and then individual NCL scripts that convert these functions into (sets of) figures. In the build up to CMIP6, the decision was made to pivot this component of the workflow into python. This allows for greater interactivity by users through notebooks and JupyterHubs, as well as greater explanation of any example cases. The repository containing these scripts are given a name of the `pmip_p2fvar_analyzer v1` (see the “Code and data availability” section).

##### 4.1 NCL

160 All the NCL scripts require the loading of a series of functions from `cvdp_data.functions.ncl`. These functions (Tab. 2) are themselves divided into three classes: those that return graphics, those that return statistics or tables, and those that are related to the identification and loading of simulation files. Combined these functions are intended to operate with an input of a directory containing all the CVDP summary files and output figures(s) or table(s) directly. All regridding and ensemble averaging is performed on the fly. Functions have been written retrospectively to output the data of these interim steps, but this is performed through an additional processing of the input directory. The plotting routines allow ‘resources’ to be passed to them, providing a high-level of control over the resulting images. These routines can also accept supra-resources, which are logical flags turning on additional functions, for example `CONSISTENCY=True` will additionally overlay hatching to indicate when the ensemble is consistent in its signal (as seen in Rehfeld et al., 2020). The NCL routines were used to make all the figures in Brierley and Wainer (2018) and Brown et al. (2020), as well as contributing the first 3 figures of Rehfeld et al. (2020).



**Table 2.** The NCL functions and procedures created to support analyses of the CVDP summary files. They are categorised according to whether they return a graphic, a statistic, or produce no output at all to the user and are intended to be called internally. **Bold** font indicates a procedure, the rest are functions.

graphics	statistics	internal
<b>plotCVDPcomparisonMaps</b>	extract_latlon_areastat	find_files_wVar
<b>plotDiffEnsMnMaps</b>	stat_ts_var	read_latlon_var
<b>plotEnsTimeseries</b>	<b>createTableGCMsExptsYears</b> <sup>†</sup>	read_diff_latlon_var
<b>plot_output_CVDPmap</b> *		find_pair_files_wVar
<b>plot_output_DiffEnsMn</b> *		read_ts
		read_ts_all
		createGCMsNameDictionary
		translateGCMsNameDictionary

\*returns a netCDF file, as well as an graphic. †returns a LaTeX formatted table.

## 170 4.2 Python

Similar to the NCL scripts, most of the analysing and plotting processes in python have been written into functions, but they are stored in different scripts according to their purposes respectively instead of being written in a single script. Each script was written in notebook format (see Sect. 4.3 for reasons) and named according to its purpose and usage, with detailed documentations available in the script. These scripts all start with a set of five functions to collect the names of available models that have the variable in the experiment and their corresponding directory and filenames respectively and return a dictionary storing these information as ""model\_name': 'directory/filename'" (hereafter referred as "target-filename dictionary"), in which function `identify_ensemble_members` requires running `find_experiment_ensemble_members.bash` in `bin` directory to identify available ensemble members (i.e. model names) whose simulations have the target variable in the experiment. Same as the NCL scripts, all regridding and ensemble averaging in python scripts is performed on the fly, and the output can be saved as either a netCDF file or a csv file based on its type, if the user requires. We also have developed a set of plotting schemes in which colours are chosen according to the colour guidelines provided by IPCC-WG1 (available at <https://github.com/IPCC-WG1/colormaps>; last assess on 17th May 2021). Some examples of possible usage are given in section 5.

## 4.3 Interactive Application

185 One advantage of the python scripts over the NCL equivalent is their wider user base. The choice of notebooks allows documentation and outputs to be stored with the scripts. A logical next step is to permit users to interact with the scripts. Attempts using Binder to create a cloud computing deployment were found to be underpowered - in part because of the two different





coding languages and any data that would want to be stored along with them. Our solution to this problem is to instead use Docker to create containerised application.

190 The Docker image contains a platform agnostic set up that can allow users to both create bespoke NCL analyses via a terminal, and act as a Jupyter notebook server to allow users to fully interact with the notebooks. The docker image is run as a minimal Linux machine inside a container on either a laptop or a cluster. It is not parallelized, so cannot run across multiple cores. However the provision of post-processed summary data means that this is not a problem, although it obviously does rule out the most sophisticated analyses. The Docker image is available at [https://github.com/pmip4/pmip\\_p2fvar\\_analyzer](https://github.com/pmip4/pmip_p2fvar_analyzer) -  
195 instructions explaining how to use it are included in the documentation at <https://pmip-p2fvar-analyzer.readthedocs.io/>.

The repository, and therefore the interactive image, contains a series of summary data of the whole ensemble, as well as a script to download the CVDP output for each individual simulation. These are a series of comma separated value tables (`data_frames` in python terminology), which collect together a single piece of information across each simulation. For example, the file `ESGF_doi.csv` contains the digital object identifier for each simulation – an important piece of information  
200 that should be included in PMIP4 publications to both improve traceability and provide due credit to those having performed the runs. We provide the long-term mean and standard deviation of the interannual timeseries of area averaged temperature and precipitation for each region identified by (Collins et al., 2013), in the `AR5_Regions` sub-directory. Statistics of the newly-incorporated regional monsoon domains (described in Sect. 3, and plotted in Fig. 7) are included in the `monsoon_domains` sub-directory. Some oft-computed metrics are tabulated in the `common_measures` sub-directory – the global mean surface  
205 temperature also includes each model's CMIP generation and effective climate sensitivity (ECS). The temperature changes averaged for 30° latitude bands over the land and ocean are included in the `tempchange_latbands` sub-directory, along with similar tables taken from the supplementary information of PMIP publications. These files form the basis of Fig 3.2b in IPCC AR6 WG1 (Eyring et al., 2021), and provide the global mean surface temperature in palaeo periods as estimated from climate models in the Technical Summary (Arias et al., 2021) and Chapter 2 (Gulev et al., 2021) in the report. The CVDP  
210 computes many different modes of variability for each simulation (Sect. 3), and the amplitudes of these are tabulated in the `climate_modes` sub-directory. For indices based on area-averaged SST, these are simply the standard deviation of the time series. For modes identified using principal component analysis, the approach of Rehfeld et al. (2020) is adopted and the amplitude is spatial standard deviation of EOF pattern averaged over same region as the analysis.

## 5 Example Uses

215 By choosing and applying appropriate functions in the scripts, the workflow can produce analyses of temperature, precipitation and monsoon (and other climatic patterns if required). These analyses can involve just the ensemble mean or individual models and return the outputs as figures (spatial maps or scatter plots etc) or data files (as `netCDF` or `csv`) as required. Detailed documentation of the scripts and functions are available elsewhere (such as in the accompanying notebooks), so will not be repeated here. Instead we provide some worked examples of outputs to help readers get an idea of the possible options. This  
220 examples have generally already featured in PMIP publications or are alluded to in them.

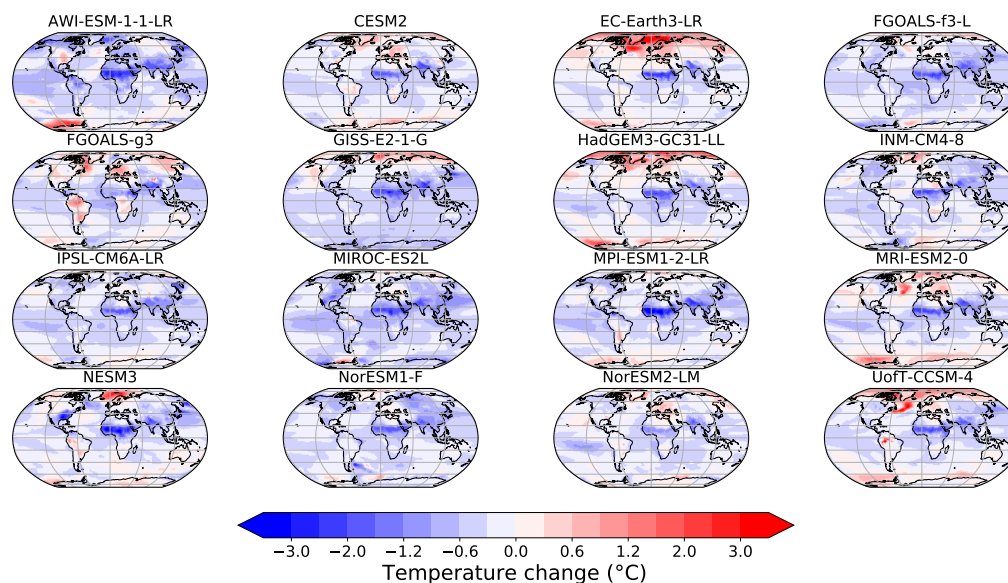


**Figure 3.** Annual mean surface temperature change ( $^{\circ}\text{C}$ ) in the *midHolocene* as simulated by individual models that features Fig. 4 and Fig. 1a in Brierley et al. (2020). Anomalies have been regridded to  $1^{\circ}$  by  $1^{\circ}$  resolution.

## 5.1 Plotting spatial patterns

The first example (Fig.3) is the annual mean temperature change in the midHolocene simulations, which shows the patterns of temperature change produced by each model in the PMIP4-CMIP6 *midHolocene* ensemble that features in Brierley et al. (2020). Fig. 3 is generated by using function `Calculation_ensemble_change('PMIP4', 'midHolocene', 'tas_spatialmean_ann', 'model')` to return a directory containing the regridded annual mean temperature change produced by each model (referred as `tas_data`) and function `plot_ensemble_tas(tas_data, 'ann')` to plot those temperature changes.

The process used to create has four major steps:

1. generate target-filename dictionaries for the *midHolocene* and the *piControl* that have the specified variable;
- 230 2. search to see which models occur in both directories, as well as the prescribed list of PMIP4 model names;
3. loop through the matching model's *midHolocene* and *piControl* simulations individually and then compute the difference (i.e. *midHolocene* - *piControl*);
4. the anomaly is regridded to  $1^{\circ}$  by  $1^{\circ}$  resolution (in order to easily calculating the ensemble mean) and then stored in the output dictionary named as the model name.

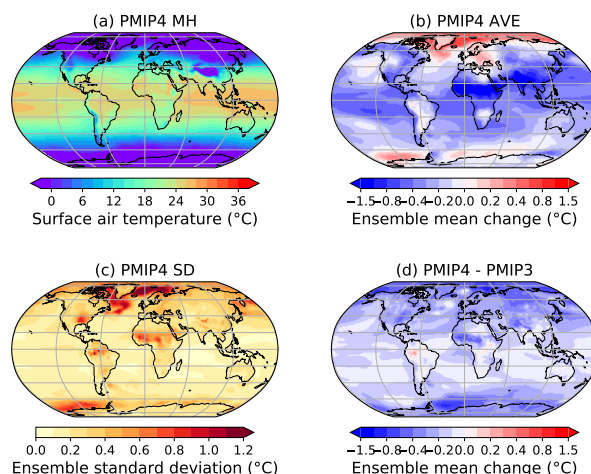


**Figure 4.** Annual mean surface temperature in the *midHolocene* simulations (°C). (a) The ensemble mean, mid-Holocene annual mean surface temperature simulated by PMIP4-CMIP6 *midHolocene* simulations. (b) The ensemble mean, annual mean temperature changes in PMIP4- CMIP6 (*midHolocene* – *piControl*) and (c) the inter-model spread, defined as the across-ensemble standard deviation. (e) The difference in the ensemble mean, annual mean temperature changes between the PMIP4-CMIP6 and the PMIP3-CMIP5. Panels (a), (b) and (c) are replotted from panels a, b and e in Fig.1 of Brierley et al. (2020) respectively.

235 The same function can be used to produce ensemble mean analysis, e.g. the ensemble mean of annual mean surface tem-  
perature in the PMIP4-CMIP6 *midHolocene* ensemble shown in Fig. 4, by entering 'mean' instead of 'model' used in  
example 1. This choice requires an additional step: calculate and return the average and the standard deviation across the  
ensemble. The NCL programmes do not have the ability to set a flag to determine whether to compute the ensemble mean  
or individual panels for each ensemble member. Instead they determine the ensemble behaviour depending on the dimension  
240 of files containing the requested input variables. If a difference plot (called using `plotDiffEnsMnMaps`) detects multiple  
files for each input, then it will compute an ensemble average of the anomalies. Should the second named experiment re-  
solve to only a single file, then the anomaly between each ensemble member and this file will be computed (this functionality  
was built to compute the ensemble mean of the biases from a single observational dataset). We provide an example code  
(`multi-panel_plot.ncl`) that was used to create Fig. 7 of Brown et al. (2020). This script also demonstrates two of  
245 the supresources: `CONSISTENCY=True` provides stippling to highlight where at least two-thirds of the ensemble members  
show the same sign of anomaly as the ensemble mean; whilst `OVERLAY_CONTROL=True` adds contour lines showing the  
ensemble mean of the variable in the second experiment named ("*piControl*" in this case.).



## 5.2 Plotting oceanic patterns – the Atlantic Meridional Overturning Circulation (AMOC)

The output files from CVDP can be used as an input for computing ensemble mean AMOC changes (mid-Holocene - piControl) in PMIP4 simulations. The variable called 'amoc\_mean\_ann', which is analysed with the modified version of CVDP for individual models, is loaded as an Iris cube for both the mid-Holocene and piControl experiments, then all models are regridded on to a  $1^\circ$  latitude grid with 61 depth levels between 0-6000m. This process is achieved through Iris cube's interpolation and regridding schemes called `iris.analysis.Linear()`. Since models can have different names for their dimension coordinates, basic cube mathematics can not be done directly. Therefore, only the regridded data in each model are extracted for calculating the differences and averages at this stage. The ensemble mean AMOC change is computed by taking the average of the regridded changes produced by individual models. After that, the model-averaged data are put back into one of the regridded models in order to use its dimension coordinates for further plotting. The figure is plotted using 'iris.quickplot' which provides a visualisation for a cube with a title, x and y labels and a colorbar where appropriate.

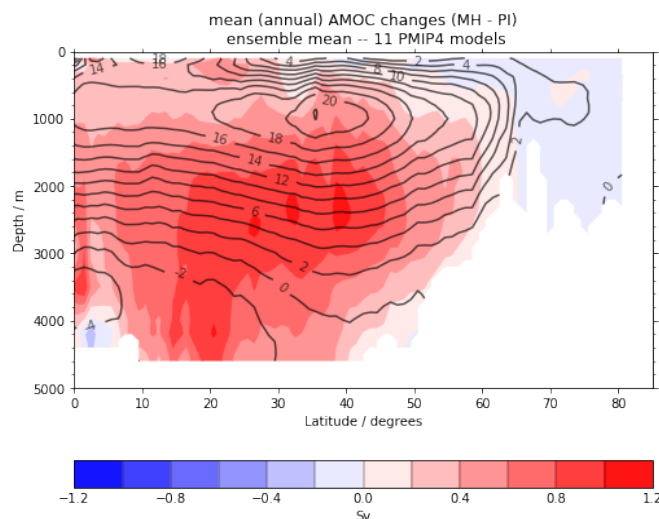


**Figure 5.** Ensemble mean plots for AMOC spatial structure changes between the midHolocene and piControl. 11 PMIP4 models which performed midHolocene experiment are used for plotting the ensemble means. The overlaid contours (black lines show AMOC strength in the piControl for locating the maximum AMOC).

In addition, the 'amoc\_mean\_ann' variable derived from the CVDP output files can also be used as an input for generating the AMOC profile for a specific latitude, e.g.  $30^\circ N$ . This is helpful when comparing the AMOC strength throughout all depths in different PMIP4 experiments, and was used to create the scatter plot of AMOC values shown in Fig. 10 of Brierley et al. (2020).

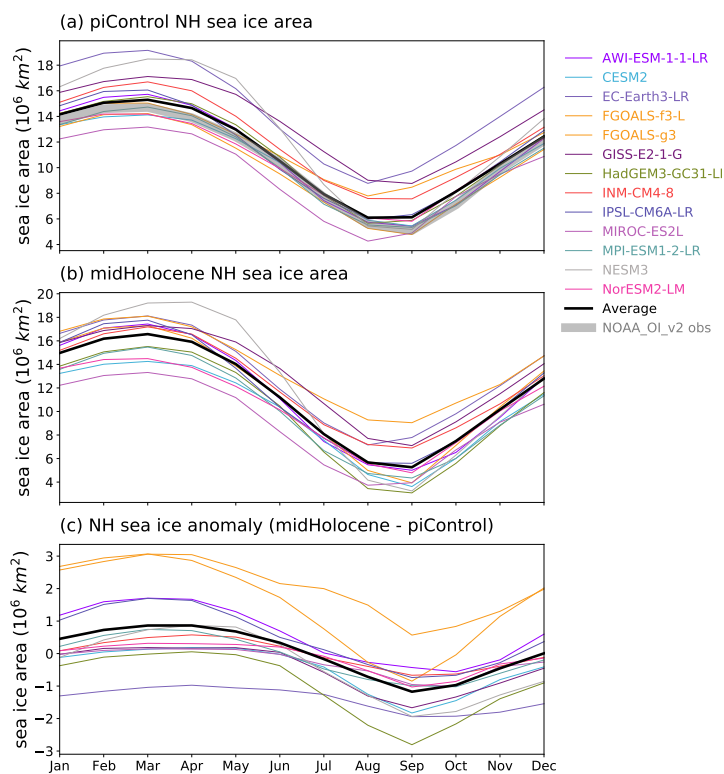


**Figure 6.** Annual cycle of the Arctic sea ice area ( $10^6 \text{ km}^2$ ) for the (a) *piControl*, (b) *midHolocene* and (c) their anomaly (*midHolocene* - *piControl*), replotted from Fig.17 of Otto-Bliesner et al. (2021). The grey contour in panel (a) shows the observed monthly mean sea ice areas from the NOAA\_OI\_v2 dataset for 1982 - 2001 (Reynolds et al., 2002).

### 5.3 Plotting time series

The CVDP is available to analyse and generate time series data. Fig 6 gives an example of the analysed results of calendar adjusted monthly mean sea ice areas (defined as sea ice fraction multiplied by the area of each grid cell) in the Arctic in the *midHolocene* and *piControl* simulations. Lines are coloured following the standard CMIP6 model colour scheme.

### 5.4 Computing statistics

Our scripts can compute statistics from the output files created by the CVDP. The simplest statistics that might be needed at the length of the data records for a particular variable. The example script `generate_model_table.ncl` interrogates the

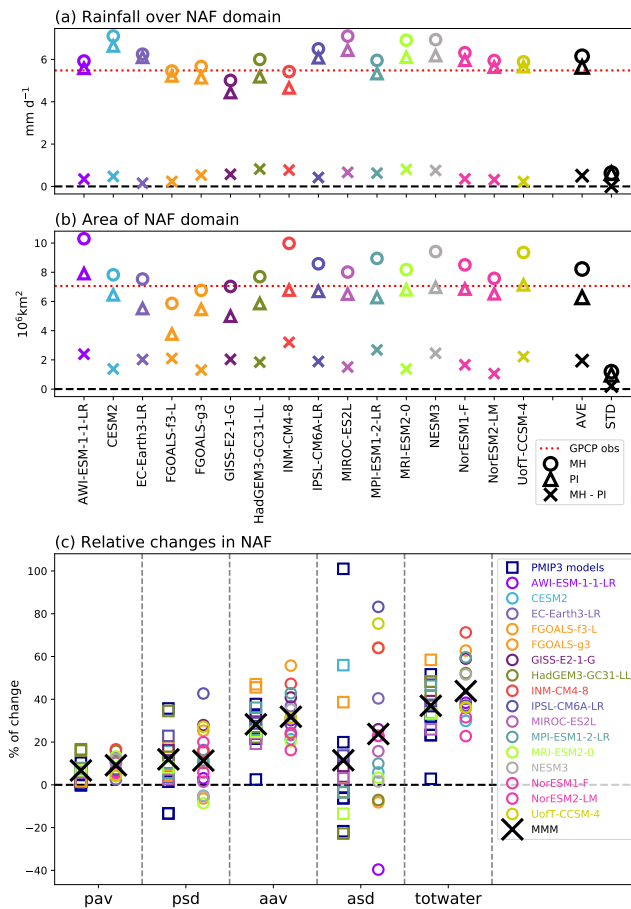


**Figure 7.** Changes in the the North African Monsoon (NAF) (a) Area-averaged NAF monsoon summer rain rate ( $\text{mm d}^{-1}$ ) in the *midHolocene* (circles) and *piControl* (triangles) simulations and the difference between them (*midHolocene* - *piControl* in crosses). (b) same as panel (a) but for the areal extent of NAF. The red dotted lines in panels (a) and (b) show the corresponded climatology seen in the 1971-2000 GPCP observational dataset (Adler et al., 2003). (c) Relative changes (Brierley et al., 2020) five different monsoon diagnostics beginning from left in order are change in area-averaged monsoon summer rain rate (**pav**), change in the standard deviation of interannual variability in the area-averaged monsoon summer rain rate (**psd**), the change in the areal extent of the NAF monsoon domain (**aav**), change in the standard deviation of interannual variability in the areal extent of the NAF monsoon domain (**asd**) and the percentage change in the total amount of water precipitated in each monsoon season computed as the precipitation rate multiplied by the areal extent (**totwater**). Colours follow the standard colours for CMIP6 models used in the IPCC AR6. If a PMIP3-CMIP5 model (square) is an earlier version of a PMIP4-CMIP6 model, it is coloured same as the PMIP4-CMIP6 one, otherwise coloured by dark blue.

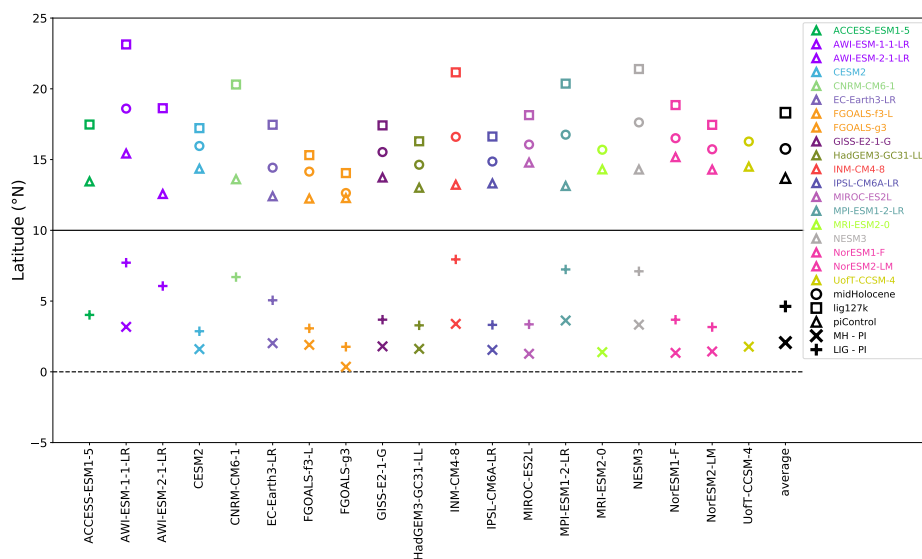


**Figure 8.** NAF expansion in the PMIP4-CMIP6 *midHolocene* and *lig127k* ensembles. The northward monsoon expansion is calculated by determining the change in latitude where the zonal mean summer (MJJAS) rain rate equals to  $2 \text{ mm d}^{-1}$  over the North Africa ( $15^{\circ}\text{W}$ – $30^{\circ}\text{E}$ )

270 directory to extract the number of years available for every simulation containing a variable called `nino34` performed under series of specified experiments. The resulting table can either be output as a spreadsheet (as comma separated values) or as in a format to be directly inputted into a  $\text{\LaTeX}$  manuscript.

Given a monthly mean precipitation netCDF file as an input, CVDP outputs time series of monsoon rainfall rate (Fig. 7a) and areal extent (Fig. 7b) of each regional land monsoon (Sect. 3). Fig. 7 is the result of this computation for the North African Monsoon. It uses these time series to compute relative changes in monsoon characteristics in the *midHolocene* experiment and shows the five available diagnostics (Brierley et al., 2020).

It is also possible to compute areal statistics from the latitude-longitude fields. As part of our modifications to the CVDP, area-averaged monthly time series for the AR5 regions are now computed for both precipitation and temperature (Sect. 3). To cope with the modification of those regions for AR6 (Iturbide et al., 2020), the area-average precipitation changes shown in Fig.3.11 of Eyring et al. (2021) are instead computed from the 2D "pr\_spatialmean\_ann" variable. An alternate approach to look at the expansion of the North African monsoon is to compute the most northerly latitude to which the monsoon reaches (as in Tab. S2 of Brierley et al., 2020). Fig. 8 gives an example of the NAF expansion in the *midHolocene* and *lig127k* ensembles. We define a series of functions to determine the change in latitude where the zonal mean summer (MJJAS) rain rate (stored



285 in the files as "monsoon\_summer\_rainrate") equals to  $2 \text{ mm d}^{-1}$  over the North Africa ( $15^{\circ}\text{W}$ – $30^{\circ}\text{E}$ ). See the corresponding notebook for details.

## 6 Summary

The simulations that have been performed for PMIP4-CMIP6, and the large amount of model output available from them, are a great resources for understanding past climates. The procedure by which this model output is analysed as an ensemble can be  
290 time-consuming and involve some methodological decisions. Here we have described the way that our group have chosen to perform our recent analyses (Brierley et al., 2020; Otto-Bliesner et al., 2021; Brierley and Wainer, 2018; Rehfeld et al., 2020; Brown et al., 2020). We document the approach used to obtain and curate PMIP4-CMIP6 simulations, process those outputs via the Climate Variability Diagnostics Package (CVDP), and then continue through to compute ensemble-wide statistics and create ensemble figures. We know from personal experience that replicating the results from published work can often involve  
295 reverse engineering the decisions made by researchers during their data processing, and that this manuscript obviates the need for such effort.

PMIP4 only exists because of the spirit of openness and cooperation within its community, which neatly combines with the IPCC's desire for greater transparency about the figures and data contained within Assessment Report 6. Through documenting our workflow here, we continue in that vein. Hopefully our efforts, such as collation of all the PMIP-related DOIs, make it  
300 easier for others to also be transparent in their research.

The main contribution of this work is not the documentation though - rather it is the provision of post-processed files for each PMIP4-CMIP6 simulation alongside scripts to readily convert them into publication ready figures and tables. The interactive application should increase further lower the barriers to analysis of palaeoclimate model research. We hope that readers are inspired with ideas of potential analyses that they themselves can perform quickly and easily by using the results of our  
305 workflow and scripts as tools to analyse PMIP4-CMIP6 simulations.

*Code and data availability.* All the codes discussed in the above workflow are available from the PMIP4 organisation on GitHub at <https://github.com/pmip4> and from Zenodo at <https://doi.org/10.5281/zenodo.5242948> (Brierley and Zhao, 2021b). The original PalCalAdjust software is at <https://github.com/pjbartlein/PaleoCalAdjust>, whilst the operational version discussed in Sect. 2 can be found at <https://github.com/pmip4/PaleoCalAdjust>. The original Climate Variability Diagnostics Package software is at <https://github.com/NCAR/CVDP-ncl>, whilst  
310 the operational version discussed in Sect. 3 can be found at <https://github.com/pmip4/CVDP-ncl>. All the scripts discussed in Sect. 4.1, Sect. 4.2 and the examples in Sect. 5 can be found within the combined repository at [https://github.com/pmip4/pmip\\_p2fvar\\_analyzer](https://github.com/pmip4/pmip_p2fvar_analyzer). These scripts, bundled with relevant data files, can be downloaded as a Docker image, to allow you to interact with them (see the documentation on the repository).

The original climate model output is available from the Earth System Grid Federation. Curated directories can be made available on request  
315 to [c.brierley@ucl.ac.uk](mailto:c.brierley@ucl.ac.uk). A subset of post-processed data is already included in the main repository at [https://github.com/pmip4/PMIP\\_past2future\\_analyzer](https://github.com/pmip4/PMIP_past2future_analyzer), which includes scripts to download the rest if required.





*Author contributions.* A.Z. and C.B. devised and wrote the manuscript. A.Z. wrote all the python scripts, documentation and the majority of the examples presented. C.B. wrote the NCL scripts. Z.Y. contributed the AMOC example. D.O. co-wrote the preliminary codes developed for the 2019 workshop at UCL, where these ideas were first explored. J. G.-D. undertook initial work on the Docker deployment and documentation creation. R.E. was responsible for creating and maintaining the curated ESGF database at UCL during the writing of Brierley et al. (2020) and Otto-Bliesner et al. (2021).

*Competing interests.* The authors declare no competing interests

*Acknowledgements.* This manuscript would not be possible without the generosity of the palaeoclimate modelling community in donating their model output. We hope that they can in turn benefit from some of the code and post-processed data that we describe here. The workflow would not exist without the development of packages by Adam Phillips, Jon Fasullo and Patrick Bartlein. We would like to thank all those in the UCL Geography, especially David Thornalley, for their support and encouragement. C.B. and R.E. were funded in part by NERC (NE/S009736/1) and a UCL Faculty Award.



## References

- Adler, R. F., Huffman, G. J., Chang, A., Ferraro, R., Xie, P.-P., Janowiak, J., Rudolf, B., Schneider, U., Curtis, S., Bolvin, D., Gruber, A., Susskind, J., Arkin, P., and Nelkin, E.: The version-2 global precipitation climatology project (GPCP) monthly precipitation analysis (1979–present), *Journal of hydrometeorology*, 4, 1147–1167, [https://doi.org/10.1175/1525-7541\(2003\)004<1147:TVGPCP>2.0.CO;2](https://doi.org/10.1175/1525-7541(2003)004<1147:TVGPCP>2.0.CO;2), 2003.
- Arias, P. A., Bellouin, N., Coppola, E., Jones, R. G., Krinner, G., Marotzke, J., Naik, V., Palmer, M. D., Plattner, G.-K., Rogelj, J., Rojas, M., Sillmann, J., Storelmo, T., Thorne, P. W., Trewin, B., Achuta Rao, K., Adhikary, B., Allan, R. P., Armour, K., Bala, G., Barimalala, R., Berger, S., Canadell, J. G., Cassou, C., Cherchi, A., Collins, W., Collins, W. D., Connors, S. L., Corti, S., Cruz, F., Dentener, F. J., Dereczynski, C., Di Luca, A., Diongue Niang, A., Doblus-Reyes, F. J., Dosio, A., Douville, H., Engelbrecht, F., Eyring, V., Fischer, E., Forster, P., Fox-Kemper, B., Fuglested, J. S., Fyfe, J. C., Gillett, N. P., Goldfarb, L., Gorodetskaya, I., Gutierrez, J. M., Hamdi, R., Hawkins, E., Hewitt, H. T., Hope, P., Islam, A. S., Jones, C., Kaufman, D. S., Kopp, R. E., Kosaka, Y., Kossin, J., Krakovska, S., Lee, J.-Y., Li, J., Mauritsen, T., Maycock, T. K., Meinshausen, M., Min, S.-K., Monteiro, P. M. S., Ngo-Duc, T., Otto, F., Pinto, I., Pirani, A., Raghavan, K., Ranasinghe, R., Ruane, A. C., Ruiz, L., Sallée, J.-B., Samset, B. H., Sathyendranath, S., Seneviratne, S. I., Sörensson, A. A., Szopa, S., Takayabu, I., Treguier, A.-M., van den Hurk, B., Vautard, R., von Schuckmann, K., Zaehle, S., Zhang, X., and Zickfeld, K.: Technical Summary, in: *Climate Change 2021: The Physical Science Basis. Contribution of Working Group I to the Sixth Assessment Report of the Intergovernmental Panel on Climate Change*, edited by Masson-Delmotte, V., Zhai, P., Pirani, A., Connors, S. L., Péan, C., Berger, S., Caud, N., Chen, Y., Goldfarb, L., Gomis, M. I., Huang, M., Leitzell, K., Lonnoy, E., Matthews, J., Maycock, T. K., Waterfield, T., Yelekçi, O., Yu, R., and Zhou, B., Cambridge University Press, 2021.
- Balaji, V., Taylor, K. E., Jukes, M., Lawrence, B. N., Durack, P. J., Lautenschlager, M., Blanton, C., Cinquini, L., Denvil, S., Elkington, M., Guglielmo, F., Guilyardi, E., Hassell, D., Kharin, S., Kindermann, S., Nikonov, S., Radhakrishnan, A., Stockhause, M., Weigel, T., and Williams, D.: Requirements for a global data infrastructure in support of CMIP6, *Geoscientific Model Development*, 11, 3659–3680, <https://doi.org/10.5194/gmd-11-3659-2018>, <https://gmd.copernicus.org/articles/11/3659/2018/>, 2018.
- Bartlein, P. J. and Shafer, S. L.: Paleo calendar-effect adjustments in time-slice and transient climate-model simulations (PaleoCalAdjust v1.0): impact and strategies for data analysis, *Geoscientific Model Development*, 12, 3889–3913, <https://doi.org/10.5194/gmd-12-3889-2019>, 2019.
- Bartlein, P. J., Harrison, S., Brewer, S., Connor, S., Davis, B., Gajewski, K., Guiot, J., Harrison-Prentice, T., Henderson, A., and Peyron, O.: Pollen-based continental climate reconstructions at 6 and 21 ka: a global synthesis, *Climate Dynamics*, 37, 775–802, <https://doi.org/10.1007/s00382-010-0904-1>, 2011.
- Braconnot, P., Harrison, S. P., Kageyama, M., Bartlein, P. J., Masson-Delmotte, V., Abe-Ouchi, A., Otto-Bliesner, B., and Zhao, Y.: Evaluation of climate models using palaeoclimatic data, *Nature Climate Change*, 2, 417–424, <https://doi.org/10.1038/nclimate1456>, 2012.
- Braconnot, P., Zhu, D., Marti, O., and Servonnat, J.: Strengths and challenges for transient Mid-to Late Holocene simulations with dynamical vegetation, *Climate of the Past*, 15, 997–1024, <https://doi.org/10.5194/cp-15-997-2019>, 2019.
- Brierley, C. and Wainer, I.: Inter-annual variability in the tropical Atlantic from the Last Glacial Maximum into future climate projections simulated by CMIP5/PMIP3, *Climate of the Past*, 14, 1377–1390, <https://doi.org/10.5194/cp-14-1377-2018>, 2018.
- Brierley, C. and Zhao, A.: PMIP\_for\_AR6\_Interactive\_Atlas, GitHub, [https://github.com/chrisbrierley/PMIP\\_for\\_AR6\\_Interactive\\_Atlas](https://github.com/chrisbrierley/PMIP_for_AR6_Interactive_Atlas), last access: 12 July 2021, 2021a.



- Brierley, C. and Zhao, A.: `pmip4/pmip_p2fvar_analyzer`: Making new release to create DOI, Zenodo,  
365 <https://doi.org/10.5281/zenodo.5242948>, last access: 24 Aug 2021, 2021b.
- Brierley, C. M., Zhao, A., Harrison, S. P., Braconnot, P., Williams, C. J. R., Thornalley, D. J. R., Shi, X., Peterschmitt, J.-Y., Ohgaito, R., Kaufman, D. S., Kageyama, M., Hargreaves, J. C., Erb, M. P., Emile-Geay, J., D'Agostino, R., Chandan, D., Carré, M., Bartlein, P. J., Zheng, W., Zhang, Z., Zhang, Q., Yang, H., Volodin, E. M., Tomas, R. A., Routson, C., Peltier, W. R., Otto-Bliesner, B., Morozova, P. A., McKay, N. P., Lohmann, G., Legrande, A. N., Guo, C., Cao, J., Brady, E., Annan, J. D., and Abe-Ouchi, A.: Large-scale features and  
370 evaluation of the PMIP4-CMIP6 *midHolocene* simulations, *Climate of the Past*, 16, 1847–1872, <https://doi.org/10.5194/cp-16-1847-2020>, <https://cp.copernicus.org/articles/16/1847/2020/>, 2020.
- Brown, J. R., Brierley, C. M., An, S.-I., Guarino, M.-V., Stevenson, S., Williams, C. J. R., Zhang, Q., Zhao, A., Abe-Ouchi, A., Braconnot, P., Brady, E. C., Chandan, D., D'Agostino, R., Guo, C., LeGrande, A. N., Lohmann, G., Morozova, P. A., Ohgaito, R., O'ishi, R., Otto-Bliesner, B. L., Peltier, W. R., Shi, X., Sime, L., Volodin, E. M., Zhang, Z., and Zheng, W.: Comparison of past and future simulations  
375 of ENSO in CMIP5/PMIP3 and CMIP6/PMIP4 models, *Climate of the Past*, 16, 1777–1805, <https://doi.org/10.5194/cp-16-1777-2020>, <https://cp.copernicus.org/articles/16/1777/2020/>, 2020.
- Christensen, J., Krishna Kumar, K., Aldrian, E., An, S.-I., Cavalcanti, I., de Castro, M., Dong, W. and Goswami, P., Hall, A., Kanyanga, J., Kitoh, A., Kossin, J., Lau, N.-C., Renwick, J., Stephenson, D., Xie, S.-P., and Zhou, T.: Climate phenomena and their relevance for future regional climate change, in: *Climate change 2013: the physical science basis. Contribution of Working Group I to the Fifth Assessment Report of the Intergovernmental Panel on Climate Change*, edited by Stocker, T., Qin, D., Plattner, G.-K., Tignor, M., Allen, S., Boschung, J., Nauels, A., Xia, Y., Bex, V., and Midgley, P., pp. 1217–1308, Cambridge University Press, 2013.  
380
- Collins, M., Knutti, R., Arblaster, J., Dufresne, J.-L., Fichefet, T., Friedlingstein, P., Gao, X., Gutowski, W. J., Johns, T., Krinner, G., Shongwe, M., Tebaldi, C., Weaver, A., and Wehner, M.: Long-term climate change: projections, commitments and irreversibility, in: *Climate Change 2013-The Physical Science Basis: Contribution of Working Group I to the Fifth Assessment Report of the Intergovernmental Panel on Climate Change*, edited by Stocker, T., Qin, D., Plattner, G.-K., Tignor, M., Allen, S., Boschung, J., Nauels, A., Xia, Y., Bex, V., and  
385 Midgley, P., pp. 1029–1136, Cambridge University Press, 2013.
- Danabasoglu, G., Yeager, S. G., Kwon, Y.-O., Tribbia, J. J., Phillips, A. S., and Hurrell, J. W.: Variability of the Atlantic meridional overturning circulation in CCSM4, *Journal of climate*, 25, 5153–5172, 2012.
- Douville, H., Raghavan, K., Renwick, J., Allan, R. P., Arias, P. A., Barlow, M., Cerezo-Mota, R., Cherchi, A., Gan, T. Y., Gergis, J., Jiang, D., Khan, A., Pokam Mba, W., Rosenfeld, D., Tierney, J., and Zolina, O.: Water Cycle Changes, in: *Climate Change 2021: The Physical Science Basis. Contribution of Working Group I to the Sixth Assessment Report of the Intergovernmental Panel on Climate Change*, edited by Masson-Delmotte, V., Zhai, P., Pirani, A., Connors, S. L., Péan, C., Berger, S., Caud, N., Chen, Y., Goldfarb, L., Gomis, M. I., Huang, M., Leitzell, K., Lonnoy, E., Matthews, J., Maycock, T. K., Waterfield, T., Yelekçi, O., Yu, R., , and Zhou, B., Cambridge University Press, 2021.  
390
- Eyring, V., Bony, S., Meehl, G. A., Senior, C. A., Stevens, B., Stouffer, R. J., and Taylor, K. E.: Overview of the Coupled Model Intercomparison Project Phase 6 (CMIP6) experimental design and organization., *Geoscientific Model Development*, 9, <https://doi.org/10.5194/gmd-9-1937-2016>, 2016.  
395
- Eyring, V., Gillett, N. P., Achuta Rao, K. M., Barimalala, R., Barreiro Parrillo, M., Bellouin, N., Cassou, C., Durack, P. J., Kosaka, Y., McGregor, S., Min, S., Morgenstern, O., and Sun, Y.: Human Influence on the Climate System, in: *Climate Change 2021: The Physical Science Basis. Contribution of Working Group I to the Sixth Assessment Report of the Intergovernmental Panel on Climate Change*, edited by Masson-Delmotte, V., Zhai, P., Pirani, A., Connors, S. L., Péan, C., Berger, S., Caud, N., Chen, Y., Goldfarb, L., Gomis, M. I., Huang,  
400



- M., Leitzell, K., Lonnoy, E., Matthews, J., Maycock, T. K., Waterfield, T., Yelekçi, O., Yu, R., , and Zhou, B., Cambridge University Press, 2021.
- 405 Fasullo, J. T., Phillips, A., and Deser, C.: Evaluation of leading modes of climate variability in the CMIP archives, *Journal of Climate*, 33, 5527–5545, <https://doi.org/10.1175/JCLI-D-19-1024.1>, 2020.
- Fox-Kemper, B., Hewitt, H. T., Xiao, C., Aðalgeirsdóttir, G., Drijfhout, S. S., Edwards, T. L., Golledge, N. R., Hemer, M., Kopp, R. E., Krinner, G., Mix, A., Notz, D., Nowicki, S., Nurhati, I. S., Ruiz, L., Sallée, J.-B., Slangen, A. B. A., and Yu, Y.: Ocean, Cryosphere and Sea Level Change, in: *Climate Change 2021: The Physical Science Basis. Contribution of Working Group I to the Sixth Assessment Report of the Intergovernmental Panel on Climate Change*, edited by Masson-Delmotte, V., Zhai, P., Pirani, A., Connors, S. L., Péan, C., Berger, S., Caud, N., Chen, Y., Goldfarb, L., Gomis, M. I., Huang, M., Leitzell, K., Lonnoy, E., Matthews, J., Maycock, T. K., Waterfield, T., Yelekçi, O., Yu, R., , and Zhou, B., Cambridge University Press, 2021.
- 410 Guiterrez, J. M., Iturbide, M., Alvarez, E. C., Diez-Sierra, J., Bedia, J., Manzanas, R., no Medina, J. B., Hauser, M., García-Díez, M., Ozge Yelecki, Felice, M. D., and Trenham, C.: PMIP4-midHolocene, GitHub, <https://github.com/IPCC-WG1/Atlas>, last access: 12 July 2021, 2021.
- 415 Gulev, S. K., Thorne, P., Ahn, J., Dentener, F., Domingues, C., Gerland, S., Gong, D., Kaufman, D., Nnamchi, H., Quaas, J., Rivera, J., Sathyendranath, S., Smith, S., Trewin, B., von Shuckmann, K., and Vose, R.: Changing State of the Climate System, in: *Climate Change 2021: The Physical Science Basis. Contribution of Working Group I to the Sixth Assessment Report of the Intergovernmental Panel on Climate Change*, edited by Masson-Delmotte, V., Zhai, P., Pirani, A., Connors, S. L., Péan, C., Berger, S., Caud, N., Chen, Y., Goldfarb, L., Gomis, M. I., Huang, M., Leitzell, K., Lonnoy, E., Matthews, J., Maycock, T. K., Waterfield, T., Yelekçi, O., Yu, R., , and Zhou, B., Cambridge University Press, 2021.
- 420 Gutiérrez, J. M., Jones, R. G., Narisma, G. T., Alves, L. M., Amjad, M., Gorodetskaya, I. V., Grose, M., Klutse, N. A. B., Krakovska, S., Li, J., Martínez-Castro, D., Mearns, L. O., Mernild, S. H., Ngo-Duc, T., van den Hurk, B., and Yoon, J.-H.: Atlas, in: *Climate Change 2021: The Physical Science Basis. Contribution of Working Group I to the Sixth Assessment Report of the Intergovernmental Panel on Climate Change*, edited by Masson-Delmotte, V., Zhai, P., Pirani, A., Connors, S. L., Péan, C., Berger, S., Caud, N., Chen, Y., Goldfarb, L., Gomis, M. I., Huang, M., Leitzell, K., Lonnoy, E., Matthews, J., Maycock, T. K., Waterfield, T., Yelekçi, O., Yu, R., , and Zhou, B., Cambridge University Press, 2021.
- 425 Harrison, S., Bartlein, P., Brewer, S., Prentice, I., Boyd, M., Hessler, I., Holmgren, K., Izumi, K., and Willis, K.: Climate model benchmarking with glacial and mid-Holocene climates, *Climate Dynamics*, 43, 671–688, <https://doi.org/10.1007/s00382-013-1922-6>, 2014.
- Harrison, S. P., Bartlein, P., Izumi, K., Li, G., Annan, J., Hargreaves, J., Braconnot, P., and Kageyama, M.: Evaluation of CMIP5 palaeo-simulations to improve climate projections, *Nature Climate Change*, 5, 735–743, <https://doi.org/10.1038/nclimate2649>, 2015.
- 430 Haywood, A. M., Tindall, J. C., Dowsett, H. J., Dolan, A. M., Foley, K. M., Hunter, S. J., Hill, D. J., Chan, W.-L., Abe-Ouchi, A., Stepanek, C., Lohmann, G., Chandan, D., Peltier, W. R., Tan, N., Contoux, C., Ramstein, G., Li, X., Zhang, Z., Guo, C., Nisancioglu, K. H., Zhang, Q., Li, Q., Kamae, Y., Chandler, M. A., Sohl, L. E., Otto-Bliesner, B. L., Feng, R., Brady, E. C., von der Heydt, A. S., Baatsen, M. L. J., and Lunt, D. J.: The Pliocene Model Intercomparison Project Phase 2: large-scale climate features and climate sensitivity, *Climate of the Past*, 16, 2095–2123, <https://doi.org/10.5194/cp-16-2095-2020>, <https://cp.copernicus.org/articles/16/2095/2020/>, 2020.
- 435 IPCC: Annex V: Monsoons [Cherchi, A., A. Turner (eds.)], in: *Climate Change 2021: The Physical Science Basis. Contribution of Working Group I to the Sixth Assessment Report of the Intergovernmental Panel on Climate Change*, edited by Masson-Delmotte, V., Zhai, P., Pirani, A., Connors, S. L., Péan, C., Berger, S., Caud, N., Chen, Y., Goldfarb, L., Gomis, M. I., Huang, M., Leitzell, K., Lonnoy, E., Matthews, J., Maycock, T. K., Waterfield, T., Yelekçi, O., Yu, R., , and Zhou, B., Cambridge University Press, 2021.



- 440 Iturbide, M., Gutiérrez, J. M., Alves, L. M., Bedia, J., Cerezo-Mota, R., Gimpeanu, E., Cofiño, A. S., Di Luca, A., Faria, S. H., Gorodetskaya, I. V., Hauser, M., Herrera, S., Hennessy, K., Hewitt, H. T., Jones, R. G., Krakovska, S., Manzananas, R., Martínez-Castro, D., Narisma, G. T., Nurhati, I. S., Pinto, I., Seneviratne, S. I., van den Hurk, B., and Vera, C. S.: An update of IPCC climate reference regions for subcontinental analysis of climate model data: definition and aggregated datasets, *Earth System Science Data*, 12, 2959–2970, <https://doi.org/10.5194/essd-12-2959-2020>, <https://essd.copernicus.org/articles/12/2959/2020/>, 2020.
- 445 Juckes, M., Taylor, K. E., Durack, P. J., Lawrence, B., Mizielinski, M. S., Pamment, A., Peterschmitt, J.-Y., Rien, M., and Sénési, S.: The CMIP6 Data Request (DREQ, version 01.00.31), *Geoscientific Model Development*, 13, 201–224, <https://doi.org/10.5194/gmd-13-201-2020>, <https://gmd.copernicus.org/articles/13/201/2020/>, 2020.
- Kageyama, M., Braconnot, P., Harrison, S. P., Haywood, A. M., Jungclauss, J. H., Otto-Bliesner, B. L., Abe-Ouchi, A., Albani, S., Bartlein, P. J., and Brierley, C.: The PMIP4 contribution to CMIP6-Part 1: Overview and over-arching analysis plan, *Geoscientific Model Development*, 11, 1033–1057, <https://doi.org/10.5194/gmd-11-1033-2018>, 2018.
- 450 Kageyama, M., Harrison, S. P., Kapsch, M.-L., Lofverstrom, M., Lora, J. M., Mikolajewicz, U., Sherriff-Tadano, S., Vadsaria, T., Abe-Ouchi, A., Bouttes, N., Chandan, D., Gregoire, L. J., Ivanovic, R. F., Izumi, K., LeGrande, A. N., Lhardy, F., Lohmann, G., Morozova, P. A., Ohgaito, R., Paul, A., Peltier, W. R., Poulsen, C. J., Quiquet, A., Roche, D. M., Shi, X., Tierney, J. E., Valdes, P. J., Volodin, E., and Zhu, J.: The PMIP4 Last Glacial Maximum experiments: preliminary results and comparison with the PMIP3 simulations, *Climate of the Past*, 17, 1065–1089, <https://doi.org/10.5194/cp-17-1065-2021>, <https://cp.copernicus.org/articles/17/1065/2021/>, 2021.
- 455 Kitoh, A., Endo, H., Krishna Kumar, K., Cavalcanti, I. F. A., Goswami, P., and Zhou, T.: Monsoons in a changing world: A regional perspective in a global context, *Journal of Geophysical Research: Atmospheres*, 118, 3053–3065, <https://doi.org/https://doi.org/10.1002/jgrd.50258>, <https://doi.org/10.1002/jgrd.50258>, 2013.
- Otto-Bliesner, B. L., Braconnot, P., Harrison, S. P., Lunt, D. J., Abe-Ouchi, A., Albani, S., Bartlein, P. J., Capron, E., Carlson, A. E., Dutton, A., et al.: The PMIP4 contribution to CMIP6-Part 2: Two interglacials, scientific objective and experimental design for Holocene and Last Interglacial simulations, *Geoscientific Model Development*, 10, 3979–4003, <https://doi.org/10.5194/gmd-10-3979-2017>, 2017.
- 460 Otto-Bliesner, B. L., Brady, E. C., Zhao, A., Brierley, C. M., Axford, Y., Capron, E., Govin, A., Hoffman, J. S., Isaacs, E., Kageyama, M., Scussolini, P., Tzedakis, P. C., Williams, C. J. R., Wolff, E., Abe-Ouchi, A., Braconnot, P., Ramos Buarque, S., Cao, J., de Vernal, A., Guarino, M. V., Guo, C., LeGrande, A. N., Lohmann, G., Meissner, K. J., Menviel, L., Morozova, P. A., Nisancioglu, K. H., O’ishi, R., Salas y Méliá, D., Shi, X., Sicard, M., Sime, L., Stepanek, C., Tomas, R., Volodin, E., Yeung, N. K. H., Zhang, Q., Zhang, Z., and Zheng, W.: Large-scale features of Last Interglacial climate: results from evaluating the *lig127k* simulations for the Coupled Model Intercomparison Project (CMIP6)–Paleoclimate Modeling Intercomparison Project (PMIP4), *Climate of the Past*, 17, 63–94, <https://doi.org/10.5194/cp-17-63-2021>, <https://cp.copernicus.org/articles/17/63/2021/>, 2021.
- 465 Phillips, A. S., Deser, C., and Fasullo, J.: Evaluating modes of variability in climate models, *Eos, Transactions American Geophysical Union*, 95, 453–455, <https://doi.org/10.1002/2014EO490002>, 2014.
- 470 Pollard, D. and Reusch, D. B.: A calendar conversion method for monthly mean paleoclimate model output with orbital forcing, *Journal of Geophysical Research: Atmospheres*, 107, 4615–ACL3–7, <https://doi.org/10.1029/2002JD002126>, 2002.
- Rehfeld, K., Hébert, R., Lora, J. M., Lofverstrom, M., and Brierley, C. M.: Variability of surface climate in simulations of past and future, *Earth System Dynamics*, 11, 447–468, <https://doi.org/10.5194/esd-11-447-2020>, <https://esd.copernicus.org/articles/11/447/2020/>, 2020.
- 475 Reynolds, R. W., Rayner, N. A., Smith, T. M., Stokes, D. C., and Wang, W.: An Improved In Situ and Satellite SST Analysis for Climate, *Journal of Climate*, 15, 1609–1625, [https://doi.org/10.1175/1520-0442\(2002\)015<1609:AIISAS>2.0.CO;2](https://doi.org/10.1175/1520-0442(2002)015<1609:AIISAS>2.0.CO;2), [https://journals.ametsoc.org/view/journals/clim/15/13/1520-0442\\_2002\\_015\\_1609\\_aiisas\\_2.0.co\\_2.xml](https://journals.ametsoc.org/view/journals/clim/15/13/1520-0442_2002_015_1609_aiisas_2.0.co_2.xml), 2002.



- Schmidt, G. A., Annan, J. D., Bartlein, P. J., Cook, B. I., Guilyardi, E., Hargreaves, J. C., Harrison, S. P., Kageyama, M., LeGrande, A. N., Konecky, B., Lovejoy, S., Mann, M. E., Masson-Delmotte, V., Risi, C., Thompson, D., Timmermann, A., Tremblay, L.-B., and Yiou, P.:  
480 Using palaeo-climate comparisons to constrain future projections in CMIP5, *Climate of the Past*, 10, 221–250, <https://doi.org/10.5194/cp-10-221-2014>, <https://www.clim-past.net/10/221/2014/>, 2014.
- Wang, B. and Ding, Q.: Global monsoon: Dominant mode of annual variation in the tropics, *Dynamics of Atmospheres and Oceans*, 44, 165–183, <https://doi.org/https://doi.org/10.1016/j.dynatmoce.2007.05.002>, <https://www.sciencedirect.com/science/article/pii/S0377026508000055>, current Contributions to Understanding the General Circulation of the Atmosphere Part 2, 2008.
- 485 Wang, B., Kim, H.-J., Kikuchi, K., and Kitoh, A.: Diagnostic metrics for evaluation of annual and diurnal cycles, *Climate dynamics*, 37, 941–955, <https://doi.org/10.1007/s00382-010-0877-0>, 2011.
- Wang, P. X., Wang, B., Cheng, H., Fasullo, J., Guo, Z. T., Kiefer, T., and Liu, Z. Y.: The global monsoon across timescales: coherent variability of regional monsoons, *Climate of the Past*, 10, 2007–2052, <https://doi.org/10.5194/cp-10-2007-2014>, <https://cp.copernicus.org/articles/10/2007/2014/>, 2014.